A low cost adaptive optics system using a membrane mirror

C. Paterson, I. Munro and J. C. Dainty

Applied Optics, The Blackett Laboratory, Imperial College of Science, Technology and Medicine, London, SW7 2BZ, UK

carlp@ic.ac.uk

Abstract: A low cost adaptive optics system constructed almost entirely of commercially available components is presented. The system uses a 37 actuator membrane mirror and operates at frame rates up to 800 Hz using a single processor. Numerical modelling of the membrane mirror is used to optimize parameters of the system. The dynamic performance of the system is investigated in detail using a diffractive wavefront generator based on a ferroelectric spatial light modulator. This is used to produce wavefronts with time-varying aberrations. The ability of the system to correct for Kolmogorov turbulence with different strengths and effective wind speeds is measured experimentally using the wavefront generator.

OCIS codes: (010.1080) Adaptive optics; (010.1330) Atmospheric turbulence

References and links

1. G. Vdovin and P. M. Sarro, "Flexible mirror micromachined in silicon," Appl. Opt. **34,** 2968–2972 (1995).
2. E. Steinhaus and S. G. Lipson, "Bimorph piezoelectric flexible mirror," J. Opt. Soc. Am. **69,** 478–481 (1979).
3. J. C. Dainty, A. V. Koryabin, and A. V. Kudryashov, "Low-order adaptive deformable mirror," Appl. Opt. **37,** 4663–4668 (1998).
4. D. Bonaccini, G. Brusa, S. Esposito, P. Salinari, P. Stefanini, and V. Biliotti, "Adaptive optics wave-front corrector using addressable liquid-crystal retarders .2.," In *Active and adaptive optical components*, Proc. SPIE **1543,** 133–143 (Osserv Astrofis Arcetri, I-50125 Florence, Italy, 1992).
5. G. D. Love, "Wave-front correction and production of Zernike modes with a liquid- crystal spatial light modulator," Appl. Opt. **36,** 1517–1524 (1997).
6. S. Restaino, D. Dayton, S. Browne, J. Gonglewski, J. Baker, S. Rogers, S. McDermott, J. Gallegos, and M. Shilko, "On the use of dual frequency nematic material for adaptive optics systems: first results of a closed-loop experiment," Opt. Express **6,** 2–6 (2000). http://www.opticsexpress.org/oearchive/source/18848.htm
7. http://okotech.com/mirrors/technical/index.html
8. R. P. Grosso and M. Yellin, "The membrane mirror as an adaptive optical element," J. Opt. Soc. Am. **67,** 399–406 (1977).
9. W. H. Press, S. A. Teukolsky, W. T. Vetterling, and B. P. Flannery, *Numerical Recipes in C*, 2nd ed. (Cambridge Univ. Press, Cambridge, 1992).
10. E. S. Claflin and N. Bareket, "Configuring an electrostatic membrane mirror by least- squares fitting with analytically derived influence functions," J. Opt. Soc. Am. A **3,** 1833–1839 (1986).
11. F. Roddier, "The problematic of adaptive optics design," in *Adaptive optics for astronomy*, D. M. Alloin and J. M. Mariotti, eds., (Kluwer Academic, 1994), pp. 89–111.
12. M. A. A. Neil, M. J. Booth, and T. Wilson, "Dynamic wave-front generation for the characterization and testing of optical systems," Opt. Lett. **23,** 1849–1851 (1998).
13. A. Glindemann, R. G. Lane, and J. C. Dainty, "Simulation of time-evolving speckle patterns using Kolmogorov statistics," J. Mod. Opt. **40,** 2381–2388 (1993).

#20597 - $15.00 US
Received March 20, 2000; Revised April 19, 2000

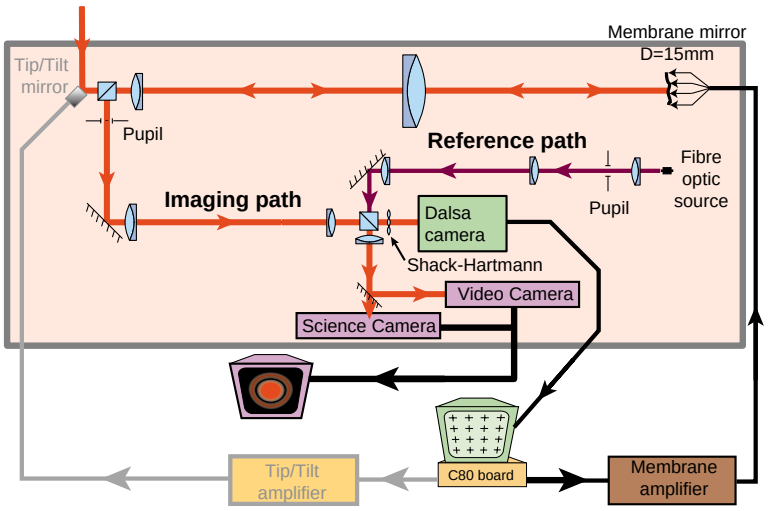

Fig. 1. Schematic of the adaptive optical system

1. Introduction

For many years the use of adaptive optics with reasonable spatial order correction and temporal bandwidths has been restricted to high budget astronomical and military applications. The primary reason has been the huge cost of such systems, with total component costs measured in hundreds of thousands of dollars and taking several years to develop and construct. For adaptive optics to find applications in other areas, such as long-distance horizontal laser beam propagation or imaging, microscopy, intra- and extra-cavity laser correction, and even amateur astronomy the costs of the systems must be reduced by several orders of magnitude. This goal is beginning to become more realizable with the recent developments in component technologies. In particular, there have been a number of advances in actuator technology specifically with the availability of relatively cheap electrostatic membrane mirrors [1], bimorph mirrors [2,3] and liquid crystal technology [4–6].

In this paper we present a low-cost closed-loop adaptive optics system which has good spatial correction (about 30 spatial orders) and high temporal bandwidth using frame rates up to 800 Hz . The system is constructed almost entirely from commercially available components, with a total component cost of about $25K. The system presented is an experimental breadboard and the emphasis in the design of the optical system has been on flexibility, allowing a number of different types of AO system components to be used in the system without redesigning.

2. System description

Figure 1 shows a schematic of the adaptive optical system. The wavefront sensor is a Shack–Hartmann type and consists of a lenslet array with 0.2 mm square lenslets of focal length 25 mm and a high speed CCD (DALSA CA-D1-0128A) 128x128 16 μm square pixels, which has a maximum frame rate of about 800 Hz.

The system has two deformable mirrors. The primary correction device in this setup is an electrostatic membrane mirror. This was supplied by TU Delft (but is commercially available [7]) and has a circular membrane of diameter 15 mm with 37 close-packed hexagonal electrodes of spacing 1.75 mm. Although it is possible to correct for tip and tilt using this membrane mirror, the amount of correction achievable is not large, and may not be sufficient for some applications, especially if there is a large amount of

#20597 - $15.00 US
Received March 20, 2000; Revised April 19, 2000

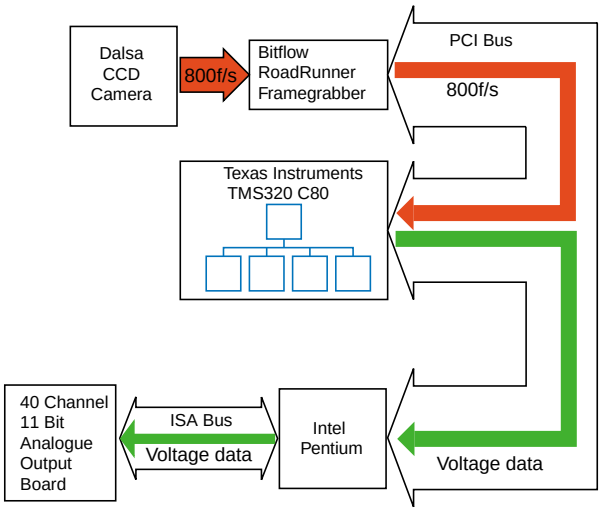

Fig. 2. Data flow for the adaptive optical system

instrument jitter on the input. Therefore the system has an additional correction mirror, a piezoelectric tip-tilt mirror (Physik Instrumente Model E610.00). In situations where the amount of tip and tilt to be corrected is not too large, the separate tip-tilt mirror can be avoided, substantially reducing the overall cost of the system. This was the case for the results presented later in this paper, where the tip-tilt mirror was not in fact used.

The deformable mirrors and the wavefront sensor all lie in planes conjugate to the entrance pupil, and since they all have different diameters, this requires a number of optical relay arms. Note also the use of a beam splitting cube just after the tip-tilt mirror in the optical path. Although not desirable in a practical AO system due to the resulting loss of light, this feature is very useful in this experimental system as it allows the use of different deformable mirrors with different optical apertures by replacing the mirror and one lens in the optical relay arm. Clearly, for a specific practical application, this beamsplitter and optical relay could be avoided, further reducing the component cost of the total system.

The system control is performed on a single Texas Instruments C80 digital signal processor board housed in a standard desktop PC (figure 2). The wavefront sensor data from the CCD camera are collected by a framegrabber (Bitflow RoadRunner) and transferred to the C80, which processes them to calculate the required actuator signals to be applied to the deformable mirrors and sends these to a 40-channel digital-to-analogue converter and low-current analogue amplifier system (Thomson-CSF). The output is recorded by video and the science camera (Starlight Xpress SX).

A reference arm in the system provides a collimated wave which is used to find easily the zero point of the wavefront sensor (i.e., the positions of the Shack–Hartmann spots on the CCD corresponding to zero aberration). Once again, for a specific application, this part of the system is not strictly necessary. However, in this experimental system, it allows the wavefront sensor to be reconfigured or replaced without lengthy alignment procedures and calculations.

3. The membrane mirror

In this system, the degree of spatial correction is limited primarily by the deformable mirrors, in particular the membrane mirror. Although membrane mirrors are not a new

#20597 - $15.00 US
Received March 20, 2000; Revised April 19, 2000

technology [8], low-cost reliable devices have only recently become available. Consequently, few AO systems to date have used membrane mirrors.

It is worth investigating in a little more detail the capability of the membrane mirror of correcting for arbitrary aberrations. The membrane mirror is a modal device, but the deformations produced by each actuator are by no means orthogonal. Additionally, because the membrane is clamped at its edge, in order to be able to correct for aberrations which are not zero at the edge of the pupil it is necessary to arrange for the optical pupil to be substantially smaller than the diameter of the membrane. Quantitative information about the ability of the membrane mirror to correct for arbitrary aberrations is necessary in order to choose the optimum optical pupil diameter and also to have some idea of the spatial correction performance one should expect from the mirror.

The membrane mirror is a curvature device whose static behaviour obeys the membrane equation [8],

$$\nabla^2 z(x,y) = -P(x,y)/T = -\epsilon_0 V^2/Td^2, \tag{1}$$

where z is the deformation, T the membrane tension and P the electrostatic pressure due to the voltage V across the gap d between the membrane and the electrode, with the boundary condition $z = 0$ at the clamped edge of the membrane. A finite element model was used to solve the linear approximation ($d \approx d_0$) of this equation, to calculate the mirror influence functions.

Performing a principal components analysis (singular value decomposition [9]) gives quantitative information about the ability of the mirror to correct for static aberrations. For a set of actuator signals represented by the vector $\mathbf{x}_\mathrm{m}$, the effect of the resulting mirror deformation on the reflected wavefront in terms of a suitable orthonormal wavefront expansion is given by

$$\boldsymbol{\phi}_\mathrm{m} = \mathbf{A}_\mathrm{m}\mathbf{x}_\mathrm{m}, \tag{2}$$

where $\mathbf{A}_\mathrm{m}$ is the influence matrix of the mirror. Conversely, the actuator signals which give the least-squares best fit to a required wavefront correction $\boldsymbol{\phi}_0$ are given by

$$\mathbf{x}_0 = \mathbf{A}_\mathrm{m}^{-1}\boldsymbol{\phi}_0, \tag{3}$$

where $\mathbf{A}_\mathrm{m}^{-1}$ is the pseudo-inverse, or least-squares inverse of $\mathbf{A}$ and is given by

$$\mathbf{A}_\mathrm{m}^{-1} = \mathbf{V}\mathbf{S}^{-1}\mathbf{U}^\mathrm{T}, \tag{4}$$

where $\mathbf{U}$, $\mathbf{S}$ and $\mathbf{V}$ are the singular value decomposition of $\mathbf{A}_\mathrm{m}$ such that $\mathbf{A}_\mathrm{m} = \mathbf{U}\mathbf{S}\mathbf{V}^\mathrm{T}$. The columns of the matrices $\mathbf{U}$ and $\mathbf{V}$ make up orthonormal sets of the mirror deformation and actuator signal spaces respectively and can be thought of as spatial modes of the system. The values of the diagonal matrix $\mathbf{S}$ are the singular values and represent the 'gains' of the different modes: a small singular value implies that a large actuator signal is required to produce unit amplitude of the given deformation mode and vice versa. Thus, these values, and in particular the ratio of the smallest to the largest value (the condition factor), give a measure of the controllability of the mirror. Modes with small singular values can have a disproportionate effect on the control matrix, resulting in large actuator signals and hence actuator clipping, and are sensitive to wavefront sensor noise. Discarding such modes may improve the controllability of the system. Fig 3 shows the singular values for the influence matrix of the TU Delft membrane mirror using different optical pupil diameters. The range of singular values is large (two and three orders of magnitude for $D = D_\mathrm{m}$ and $D = 0.5D_\mathrm{m}$ respectively). Although it is necessary to choose an optical pupil smaller than the membrane diameter to allow for non-zero

#20597 - $15.00 US Received March 20, 2000; Revised April 19, 2000

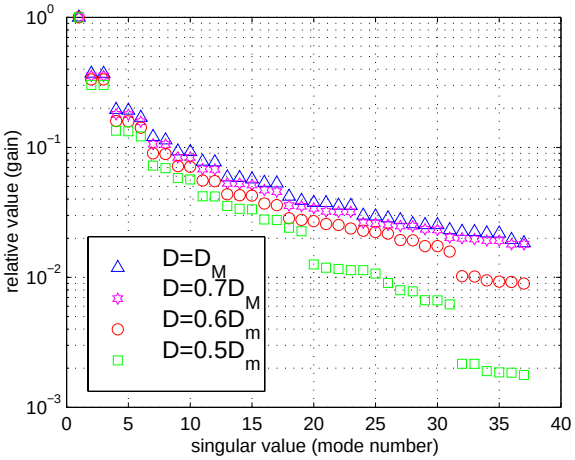

Fig. 3. Singular values of the membrane mirror influence matrix

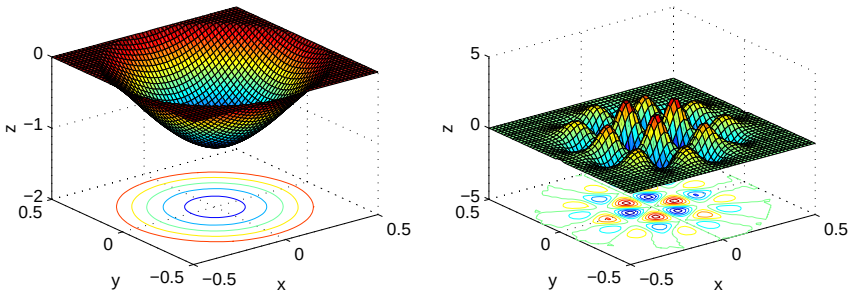

(a) Mode 1 (b) Mode 37

Fig. 4. Two modes of the membrane mirror corresponding to the largest (mode 1) and smallest (mode 37) singular values.

phase at the edge of the pupil [10], the range of the singular values is larger for the smaller optical pupil diameters. Fig 4 shows the membrane deformation corresponding to the largest and smallest singular values for the case $D = D_{\mathrm{m}}$.

3.1. *Accounting for the aberration statistics*

Of course, whether or not a given spatial mode in the system is likely to swamp the control matrix, leading to clipping, will depend on a large extent on the spatial mode content of the wavefront aberrations to be corrected. For example, for phase aberrations with Kolmogorov statistics, the power spectrum of the phase variations varies as $|k|^{-11/3}$. This will give a weighting to the expected magnitudes of the various mirror modes required for aberration compensation. To get a better idea of the controllability of the membrane for specific types of aberration, it is useful to include these statistics in the analysis. If the Kahunen–Loève [11] expansion is chosen for the orthonormal wavefront expansion, then the covariance of $\boldsymbol{\phi}$ denoted $\mathbf{C} = \langle \boldsymbol{\phi}\boldsymbol{\phi}^{\mathrm{T}} \rangle$ is diagonal. Furthermore, multiplying the wavefront expansion by $\mathbf{C}^{-1/2}$ gives a vector $\mathbf{C}^{-1/2}\boldsymbol{\phi}$, which has a covariance equal to the identity matrix. Taking these weights for the different modes of the expansion into account in the influence matrix, Eq. (2) describing the mirror

#20597 - $15.00 US
Received March 20, 2000; Revised April 19, 2000

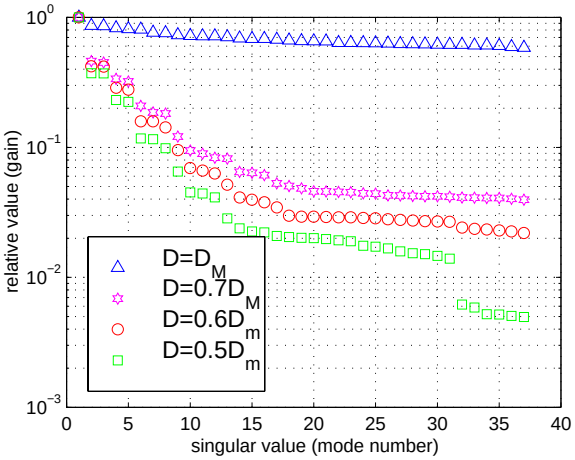

Fig. 5. Singular values of the membrane mirror influence matrix weighted for Kolmogorov statistics

deformations becomes

$$\mathbf{C}^{-1/2}\boldsymbol{\phi} = (\mathbf{C}^{-1/2}\mathbf{A}_{\mathrm{m}})\mathbf{x} \tag{5}$$

A singular value decomposition of the weighted influence matrix $\mathbf{C}^{-1/2}\mathbf{A}_{\mathrm{m}}$ gives a better measure of the controllability of the mirror for wavefront aberrations of these statistics. Fig 5 shows the singular values for the influence matrix weighted for Kolmogorov statistics. The ranges of singular values are reduced compared with those for the unweighted matrix, particularly for the larger optical pupil sizes, suggesting that the spatial response of the mirror is suited to correction of Kolmogorov aberrations.

This is no surprise given the curvature behaviour of the mirror. In such a system, where the actuators control directly the second derivative of the local deformation, one would expect the available amplitude of deformation for a given spatial frequency k to vary with k^{-2}. This is in fact very similar to the Kolmogorov power law where the typical amplitude of the aberrations varies with $k^{-11/6}$.

3.2. *Numerical Modelling*

The ability of the mirror to correct for static aberrations with Kolmogorov statistics has been investigated using Monte-Carlo simulation. Monte-Carlo was chosen to take into account the strongly non-linear effect of actuator signal clipping. For a given aberrated wavefront $\boldsymbol{\phi}_0$, using least-squares correction, and clipping the actuator signals to their maximum permissible values with the limiting function $L(\mathbf{x})$, the residual wavefront error (fitting error) is given by

$$\boldsymbol{\phi}_{\mathrm{e}} = \mathbf{A}_{\mathrm{m}} L(\mathbf{A}_{\mathrm{m}}^{-1}\boldsymbol{\phi}_0) - \boldsymbol{\phi}_0 \tag{6}$$

where the limiting function $L(\mathbf{x})$ is given by

$$L(\mathbf{x}) = \begin{cases} x & |x| \le x_{\max} \\ x_{\max} x/|x| & |x| > x_{\max} \end{cases} \tag{7}$$

and where $x_{\max}$ is the maximum actuator signal permissible. The piston term, which has no effect on the image, was ignored throughout by excluding it from the basis used

#20597 - $15.00 US
Received March 20, 2000; Revised April 19, 2000

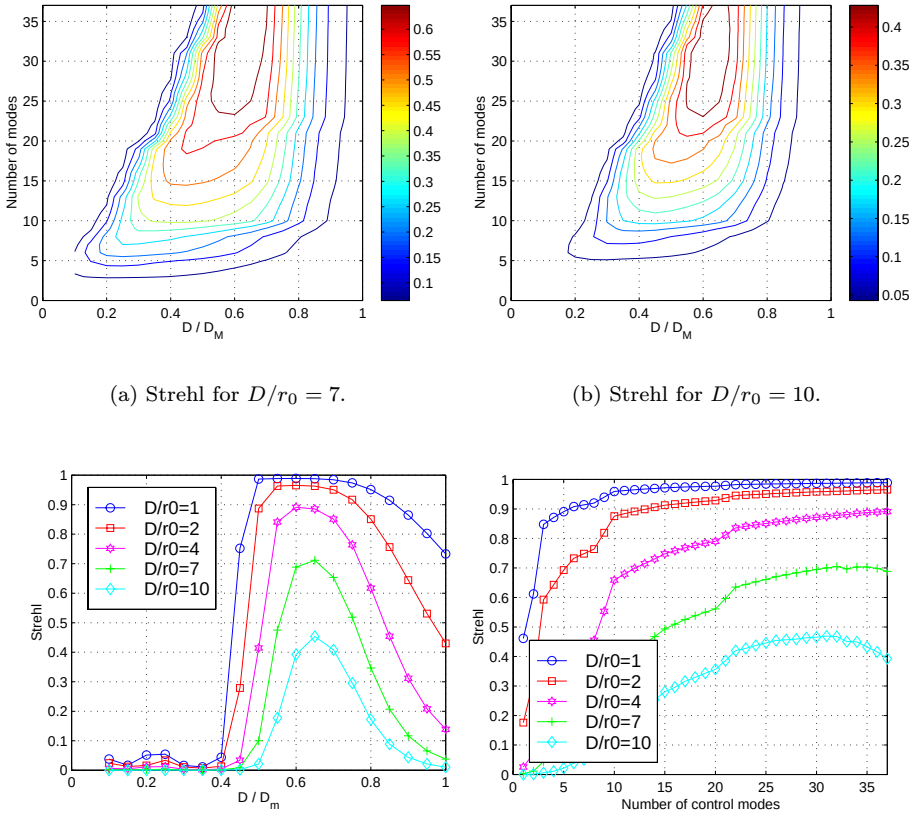

(a) Strehl for $D/r_0 = 7$.

(b) Strehl for $D/r_0 = 10$.

(c) Strehl v. optical pupil (all modes)

(d) Strehl v. number of spatial modes (for $D = 0.6D_{\mathrm{m}}$)

Fig. 6. Mean Strehl, $S = \exp(-\sigma^2)$, correcting for Kolmogorov turbulence using the membrane mirror. (Monte Carlo with $\lambda = 633\,\mathrm{nm}$, maximum actuator voltage $V_{\max} = 200\,\mathrm{V}$, maximum membrane deflection was $7.5\,\mu\mathrm{m}$ with all electrodes set to $V_{\max}$).

to expand the wavefront. Then, the residual wavefront variance over the aperture is given by

$$\sigma_{\mathrm{e}}^2 = \left\langle \phi_{\mathrm{e}}^2 \right\rangle = \boldsymbol{\phi}_{\mathrm{e}}^{\mathrm{T}} \boldsymbol{\phi}_{\mathrm{e}} \tag{8}$$

Results of the Monte-Carlo simulations to model the correction of Kolmogorov aberrations with strengths $D/r_0 = 7$ and $D/r_0 = 10$ with the TU Delft mirror are shown in Fig 6. Figures 6(a) and (b) show the effect of the choice of the optical pupil diameter and the number spatial correction modes (discarding those modes with the smallest singular values) on the mean Strehl, when using the mirror to correct aberrations with Kolmogorov statistics for two strengths. The approximation $S = \exp(-\sigma_{\mathrm{e}}^2)$, is used to estimate the Strehl. The optimum choice of optical pupil diameter is about $D = 0.65D_{\mathrm{m}}$. Figures 6(c) and (d) show respectively the effects of the choice of optical pupil size and of the number of spatial control modes in the control matrix, discarding those with the smallest singular values. Discarding modes at the higher aberration strengths increases the Strehl achievable. Note that this is not a result of wavefront sensor noise, which

#20597 - $15.00 US
Received March 20, 2000; Revised April 19, 2000

this model does not account for, but is a result of actuator clipping which is more pronounced at the higher aberration strengths. The effect of wavefront sensor noise will be greatest for spatial modes with the smallest singular values (since they result in modes with large gains in the control matrix) and is likely to degrade performance with large numbers of modes further. The results show, however, that it should be possible to achieve reasonable correction (Strehl ratio of 0.7) for Kolmogorov turbulence with $D/r_0 = 7$ using the 37 actuator membrane mirror.

4. System Operation

The AO system control is very elementary, the spatial and temporal aspects being treated separately. The spatial control matrix is calculated online in a calibration run with a static (aberrated) point source input. Each mirror actuator signal is varied in turn, the resulting change to the wavefront sensor signal recorded and the actuator–sensor interaction matrix for the system built up. The control matrix is calculated as a least squares pseudoinverse of the interaction matrix, discarding a number of modes corresponding to those with the smallest singular values. Thus the spatial control does not make full use of the statistics of the aberrations to be corrected.

The temporal control is a simple integrator. The actuator signals for the nth iteration of the control loop are given by

$$\mathbf{x}_n = (1 - \beta)\mathbf{x}_{n-1} + g\mathbf{M}\mathbf{s}_n \tag{9}$$

where g is the integrator gain, $\mathbf{M}$ is the spatial control matrix, $\mathbf{s}$ is the sensor signal and β ($\beta \ll 1$)is a bleed parameter included to make the system resistant to possible modes of the mirror which are invisible to the wavefront sensor. In fact we have not seen any evidence of such modes in the system, which is probably attributable to the unmatched nature of the mirror–sensor system. A curvature wavefront sensor would be better matched to the membrane mirror. Suitable values for the temporal control loop parameters were found by trial end error.

5. System Performance

The performance of the AO system has been investigated using a dynamic wavefront generator based on a 256x256 pixel ferroelectric spatial light modulator operating as a first-order diffractive optical element [12]. Time varying wavefronts were generated corresponding to a point source viewed through a single frozen layer (Taylor hypothesis) of turbulence with quasi-Kolmogorov spatial statistics moving across the input aperture.[1] The video (Fig 7) shows a sample of the dynamic behaviour of the system when correcting for these wavefronts.

The ability of the AO system to correct for these dynamic aberrations was measured for different turbulence strengths and speeds characterized respectively by the quantities D/r_0 and v/r_0, where r_0 is the Fried parameter, D the input aperture diameter and v the speed which the frozen turbulence layer moves across the input aperture, i.e., the wind speed. Long exposures recorded with the science camera were used to calculated the Strehl ratio of the corrected and uncorrected output images.

Fig 8 shows the effect of discarding different numbers of spatial modes from the system control matrix. The optimum number of modes is about 25 (which corresponds

[1] In fact the turbulent screens generated are not pure Kolmogorov in nature. Since they are generated as the inverse discrete Fourier transform of sampled Kolmogorov spectra [13], they are in fact sections of larger periodic screens and thus have a finite outer scale L_0. This has the effect of reducing slightly the amplitude of the low spatial frequencies. This in turn has very little effect on the temporal behaviour as far as testing the dynamical behaviour of the AO system is concerned, the greatest effect being to reduce slightly the amplitude of tip and tilt correction required.

#20597 - $15.00 US Received March 20, 2000; Revised April 19, 2000

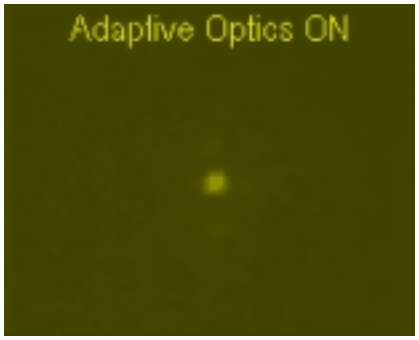

Fig. 7. Video showing the output image with the adaptive optics system correcting for turbulence with D/r_0=6 and v/r_0=25 Hz (nominal). (1.89Mb movie)

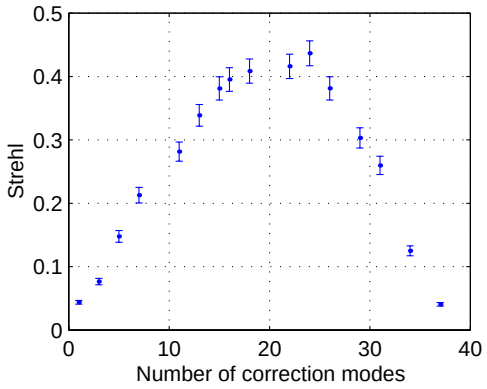

Fig. 8. Plot of Strehl ratio v. number of spatial modes. [Exposure time 4 seconds, D/r_0=6, v/r_0=25 Hz (nominal)]

#20597 - $15.00 US
Received March 20, 2000; Revised April 19, 2000

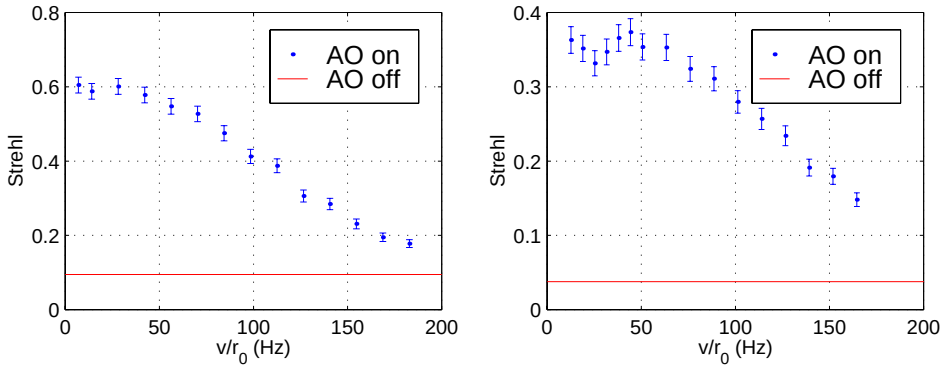

(a) Strehl for $D/r_0 = 5$.

(b) Strehl for $D/r_0 = 9$.

Fig. 9. Experimental performance of the AO system for quasi-Kolmogorov turbulence of different strengths and wind speeds. ($g = -0.52$, frame rate $= 800\,\mathrm{s}^{-1}$, 24 spatial correction modes)

to a condition factor of about 0.13 for the control matrix). As more modes are included, wavefront sensor noise and actuator clipping degrade performance. In fact using all the available spatial modes results in performance no better than using just one. Note that the decline in performance as the number of spatial modes is increased above the optimum is much steeper than that predicted by the model of the mirror alone. There are several reasons for this. The results of Fig 6(d) take no account of wavefront sensor deficiencies, i.e., the unsensed component of the aberration and sensor noise. Also, in practice, the mirror is not initially flat, which reduces the effective actuator range available for correction of turbulence.

Fig 9 shows the performance of the system as a function of the normalized wind speed (v/r_0), for two different strengths (D/r_0). For small v/r_0, the Strehl ratio achieved is in agreement with that predicted for the mirror by the static model [Fig 6(d)]. Also note that considerable improvement to the Strehl ratio is achieved even with normalized wind speeds v/r_0 in excess of 100 Hz

The closed-loop bandwidth of the system was measured by recording the residual wavefront sensor signal variances for sinusoidal input signals. Fig 10 plots the ratio of the sensor signal variances for the AO system off and on (averaged over all the sensor signals) for different frequency input signals. The unit gain crossover occurs at about 50 Hz.

6. Conclusions

A low cost high speed adaptive optical system using a 37 actuator electrostatic deformable mirror and running on a single digital signal processor has been demonstrated. Numerical modelling of the mirror were carried out to determine the optimum active optical diameter of the mirror and the effect of the number of spatial modes used on the fitting performance of the mirror. The performance of the system has been investigated in detail experimentally using a dynamic wavefront generator, which was used to produce time varying optical aberrations corresponding to Kolmogorov turbulence with well defined parameters. For slowly varying turbulence, the Strehl ratios achievable with the system agree with the predictions made from static modelling of the membrane

#20597 - $15.00 US
Received March 20, 2000; Revised April 19, 2000

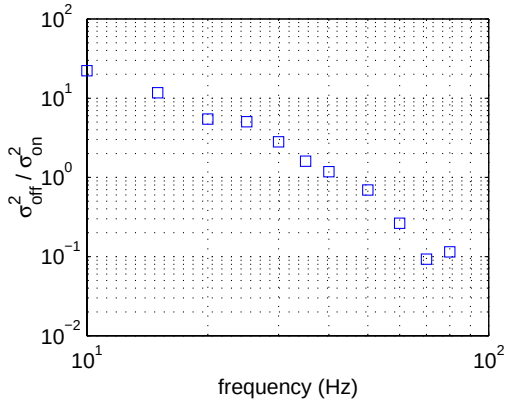

Fig. 10. The ratio of the measured wavefront sensor signal variances for the AO system off and on for sinusoidally varying input signals.

mirror. Improvement to the Strehl ratio was achieved for normalized wind speeds (v/r_0) in excess of 100 Hz. It has been demonstrated experimentally that the performance of the system can be improved by discarding a number of spatial modes from the system control matrix. There are still a number of improvements which could be made to the system's spatial and temporal control. In particular, the temporal control of the system is far from optimal and it is expected that optimization of this this should give considerable improvements to the closed-loop bandwidth of the system.

The system is comprised almost entirely of commercially available components with a total cost of about $25K, a cost which could be reduced further if the flexibility of the system were to be sacrificed for a particular application. The relatively low cost of the system shows that adaptive optics with good spatial correction is feasible for non-astronomical applications.

Acknowledgements

This work was funded by the UK EPSRC under grant GR/M46846 with additional support from Spectron Laser Systems, Pilkington Optronics and the EU (MOSIS: ESPRIT project No. 31063).

#20597 - $15.00 US
Received March 20, 2000; Revised April 19, 2000